IJCRT.ORG ISSN : 2320-2882

INTERNATIONAL JOURNAL OF CREATIVE RESEARCH THOUGHTS (IJCRT)

An International Open Access, Peer-reviewed, Refereed Journal

# Intelligent Method Based On Decoding Psychological Emotional States

[1]Dr.K.Ambedkar, [2]Buru Nithin

[1]Associate Professor, [2]IV B.Tech Student

[1]Department of CSE(Data Science)

[1]Geethanajli College of Engineering and Technology, Hyderabad, India

***Abstract:*** Current artificial intelligence systems are limited by their passive execution of commands, lacking autonomous perception, learning, and emotional understanding, which restricts their universality. To address this, we developed a novel electroencephalography (EEG)-based psychological emotion state decoding method, combining singular spectrum analysis and entropy measures. By implementing vector dissimilarity criteria to accelerate entropy calculations and employing a dynamic sample entropy model, we enhanced the computational efficiency and cognitive computation of emotional states. Our results demonstrate a significant improvement in computational efficiency, achieving an average recognition accuracy of 82.78±16.22% for positive and negative emotions, and a peak accuracy of 84.64% in within-individual recognition. Furthermore, cross-individual recognition of positive, neutral, and negative states yielded 64.15% accuracy. These findings indicate that our proposed emotion recognition method exhibits superior universality and generalization, effectively identifying human psychological and emotional states.

***Index Terms*** - EEG Decoding, Electroencephalography (EEG), Cognitive Computing Brain Activity Fourier Transform**.**

## 1.INTRODUCTION

The ability to accurately decode human emotions is critical for the development of truly intelligent machines. This interdisciplinary research area, drawing from psychology, cognitive science, and computer science, forms the foundation for emotional artificial intelligence. However, current sentiment analysis faces significant challenges, including data imbalance, linguistic diversity, and the inherent complexity of emotional expression (Ghasemi et al., 2024; Pandya et al., 2024; Liu et al., 2022; Movassagh et al., 2021; Usman & Abdullah, 2023). While external emotional signals like facial expressions and voice intonation are easily observed, they are susceptible to subjective and social influences. Physiological signals, such as electroencephalography (EEG), offer a more objective window into emotional states, mitigating these biases (K Liu et al., 2023). Yet, the significant individual variability in physiological emotional responses poses a substantial hurdle, limiting the universality and robustness of current recognition models (Lu et al., 2021; S Liu et al., 2023). To address this, we propose a novel EEG decoding method based on Singular Spectrum Analysis (SSA) and entropy measures, aiming to endow cognitive computing systems with human-like emotional cognition. This method optimizes entropy feature extraction using SSA decomposition, accelerates entropy calculation through vector dissimilarity judgment, and enhances generalization through dynamic entropy measure representation. By integrating entropy measurement with machine learning, high accuracy auditory attention object identification from EEG signals is achieved. This research offers three key contributions: a novel EEG decoding method with optimized performance, a fast entropy calculation technique, and enhanced generalization for cross-individual emotional state recognition. This paper is

structured as follows: Section 1 reviews current emotion recognition methods; Section 2 details the proposed cognitive computing-based decoding approach; Section 3 presents performance validation; and Section 4 concludes.

## 2. Calculation method of psychological emotional states

This research investigates the factors affecting EEG decoding performance using entropy measures, leading to the development of a novel algorithm that integrates Singular Spectrum Analysis (SSA). To accelerate entropy calculations, a rapid computation method utilizing vector dissimilarity criteria is proposed.

Brain activity manifests as electrical signals, detectable on the scalp as EEG. Analyzing these signals allows for the interpretation of various brain states. With the rise of machine learning in biomedicine, EEG decoding has advanced significantly, effectively isolating task-related brain activity (Cao et al., 2023). The fundamental EEG decoding process involves signal acquisition, preprocessing, and feature extraction, as illustrated in Fig. 1.

EEG signals, characterized by non-stationarity, nonlinearity, and complexity, often require advanced processing for effective decoding. Direct entropy feature extraction can be insufficient. To improve decoding, techniques like wavelet transforms, empirical mode decomposition, and short-time Fourier transforms are utilized. In our approach, EEG decoding using entropy measures involves two steps: first, time-series decomposition and reconstruction via Singular Spectrum Analysis (SSA), and second, entropy feature extraction from the resulting components. This method enhances feature information and improves decoding performance.

SSA, a nonlinear time-series analysis based on principal component analysis, analyzes time-series dynamics and constructs a trajectory matrix through phase space reconstruction (Ly & El-Sayegh, 2023). Singular Value Decomposition (SVD) then decomposes this matrix into key component structures. Given EEG's non-stationary and random nature, SSA is well-suited for its analysis. By integrating SSA decomposition and reconstruction, we isolate relevant EEG time-series components, facilitating subsequent entropy feature extraction. This integration forms the basis of our novel EEG decoding algorithm, shown in Fig. 2.

The SSA method consists of decomposition and reconstruction phases. Decomposition involves embedding and SVD. A phase reconstruction algorithm maps a one-dimensional time series, t(n), into a trajectory matrix, X, as shown in Eq. (1), where w is the window length.

X = [ t(1) t(2) ... t(L) ]
[ t(2) t(3) ... t(L+1)]
[ ... ... ... ... ]
[ t(w) t(w+1) ... t(N) ]

SVD then decomposes X into a sum of elementary matrices, as shown in Eq. (2), where λj are eigenvalues, Uj are eigenvectors, and Vj is derived from XTUj.

X = Σ(w, j=1) √(λj) * Uj * Vj^T = X1 + X2 + ... + Xw

Reconstruction involves grouping and diagonal averaging. Singular values and their corresponding eigenvectors are grouped, forming matrices Xck. Subsets are created, and the final reconstructed matrix, $\tilde{X}$, is obtained by summing these grouped matrices.

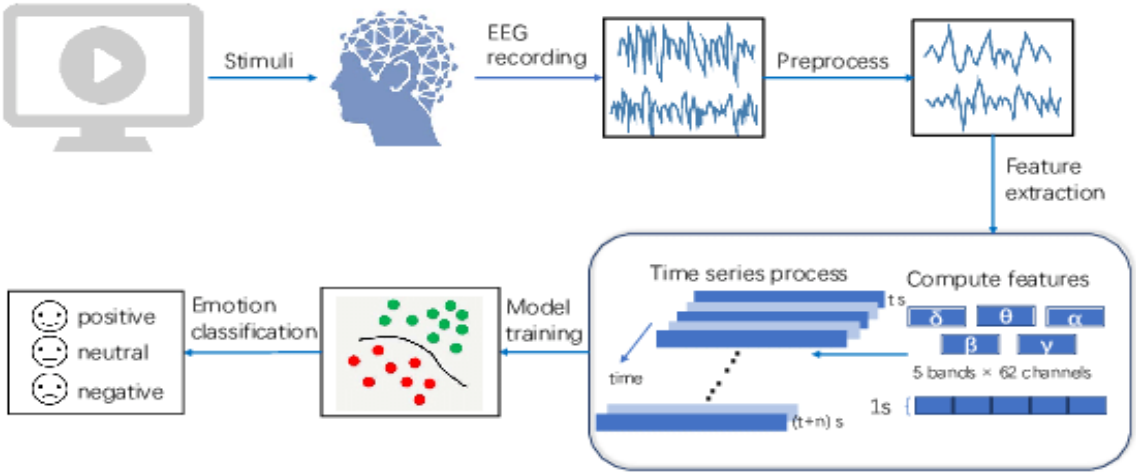


Fig. 1. Basic flow of emotional state decoding based on EEG signal.

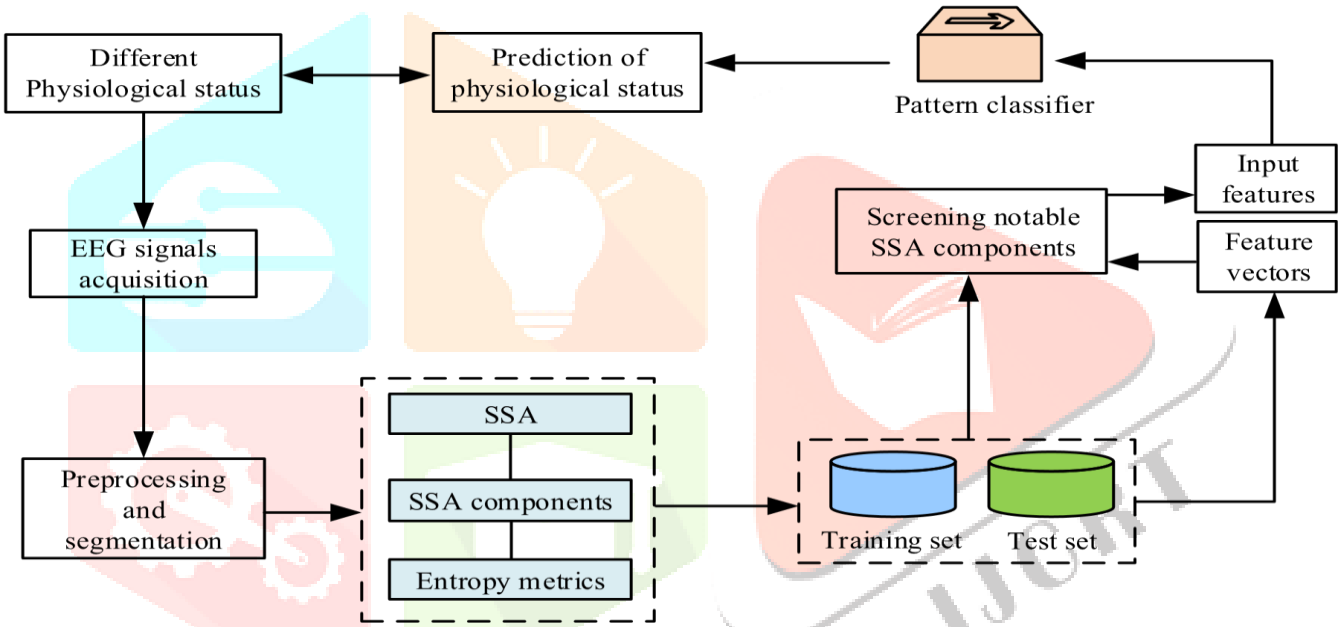


Fig. 2. Basic flow of EEG decoding based on SSA and entropy measure.

The reconstructed matrix, $\tilde{X}$, with dimensions w × L, can be represented as $\tilde{X} = \tilde{}(x)i,j$, where $1 \le i \le w$ and $1 \le j \le L$. Diagonal averaging within the SSA reconstruction process involves averaging the elements $\tilde{}(x)i,j$ along the diagonal i + j = n + 1 of the matrix. This yields the reconstructed time series y(n), for n = 1, 2, 3, ..., N, defined mathematically by Eq. (3):

$$y(n) = \begin{cases} (1/n) * \Sigma(i=1 \text{ to } n) \tilde{} xi,n-i+1, & 1 \le n \le w \\ (1/w) * \Sigma(i=1 \text{ to } w) \tilde{} xi,n-i+1, & w \le n \le L \\ (1/(N-n+1)) * \Sigma(i=n-L+1 \text{ to } w) \tilde{} xi,n-i+1, & L + 1 \le n \le N \end{cases}$$

The reconstructed time series y(n) corresponds directly to the elements of the matrix $\tilde{X}$. In the grouping phase of SSA reconstruction, if k = w, then $X = \tilde{X}$. In this scenario, the original time series t(n) can be fully reconstructed from matrix X. The time series can be expressed as the sum of individual one-dimensional time series, as shown in Eq. (4):

$$t(n) = \Sigma(ck=1 \text{ to } w) \tilde{} yck(n), \quad \Sigma(n=1 \text{ to } N)$$

To enhance EEG entropy information extraction and improve decoding, this study integrates SSA processing into the entropy measurement feature extraction. Given an EEG time series s(n), for n = 1, 2, 3, ..., N, the time

trajectory matrix is formed through phase space reconstruction, varying the window length w. Singular Value Decomposition (SVD) then yields eigenvalues and corresponding left and right singular vectors, used to reconstruct SSA components of various orders. Finally, the EEG signal s(n) is represented as the sum of these SSA components.

Fig. 3 illustrates the process of brain entropy feature extraction using SSA components from EEG signals. The SSA algorithm, comprising phase-space reconstruction, SVD, grouping, and diagonal averaging, is employed to process EEG and generate SSA components for each order. As each SSA component is a one-dimensional time series, their entropy measures provide information about the EEG signal. Four distinct entropy measurement techniques—Multi-scale, Sample, Fuzzy, and Approximate Entropy—are utilized to analyze these EEG signals, extracting specific features.

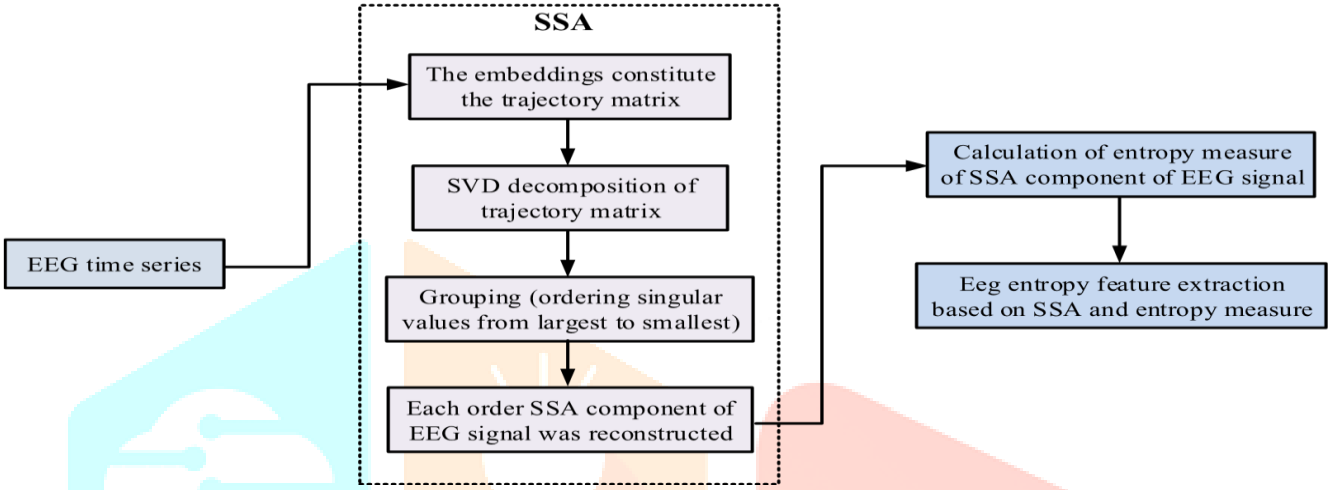


Fig. 3. EEG entropy feature extraction based on SSA components of EEG signals.

The reconstructed matrix, $\tilde{X}$, with dimensions w × L, can be represented as $\tilde{X} = \tilde{}(x)i,j$, where $1 \le i \le w$ and $1 \le j \le L$. Diagonal averaging within the SSA reconstruction process involves averaging the elements $\tilde{}(x)i,j$ along the diagonal i + j = n + 1 of the matrix. This yields the reconstructed time series y(n), for n = 1, 2, 3, ..., N, defined mathematically by Eq. (3):

$$y(n) = \begin{cases} (1/n) * \Sigma(i=1 \text{ to } n) \tilde{} xi,n-i+1, & 1 \le n \le w \\ (1/w) * \Sigma(i=1 \text{ to } w) \tilde{} xi,n-i+1, & w \le n \le L \\ (1/(N-n+1)) * \Sigma(i=n-L+1 \text{ to } w) \tilde{} xi,n-i+1, & L+1 \le n \le N \end{cases}$$

The reconstructed time series y(n) corresponds directly to the elements of the matrix $\tilde{X}$. In the grouping phase of SSA reconstruction, if k = w, then $X = \tilde{X}$. In this scenario, the original time series t(n) can be fully reconstructed from matrix X. The time series can be expressed as the sum of individual one-dimensional time series, as shown in Eq. (4):

$$t(n) = \Sigma(ck=1 \text{ to } w) \tilde{} yck(n), \quad \Sigma(n=1 \text{ to } N)$$

To enhance EEG entropy information extraction and improve decoding, this study integrates SSA processing into the entropy measurement feature extraction. Given an EEG time series s(n), for n = 1, 2, 3, ..., N, the time trajectory matrix is formed through phase space reconstruction, varying the window length w. Singular Value Decomposition (SVD) then yields eigenvalues and corresponding left and right singular vectors, used to reconstruct SSA components of various orders. Finally, the EEG signal s(n) is represented as the sum of these SSA components.

Fig. 3 illustrates the process of brain entropy feature extraction using SSA components from EEG signals. The SSA algorithm, comprising phase-space reconstruction, SVD, grouping, and diagonal averaging, is employed to process EEG and generate SSA components for each order. As each SSA component is a one-dimensional time series, their entropy measures provide information about the EEG signal. Four distinct

entropy measurement techniques—Multi-scale, Sample, Fuzzy, and Approximate Entropy—are utilized to analyze these EEG signals, extracting specific features."identified as "relevant features" in a specific

Following feature extraction, a critical step in EEG decoding involves identifying and removing irrelevant features. To achieve this, relevant features are selected within a specific feature vector space for each EEG task. Irrelevant dimensions are eliminated through dimensionality reduction. In this study, pairwise t-tests, with a significance level of $p = 0.05$, are used to conduct feature selection on the SSA components of the EEG. This process isolates entropy features with statistically significant differences, which are subsequently used for EEG signal decoding.

### 3.2. Emotion Recognition Cognition: Computational Methods

EEG entropy measures, reflecting the nonlinear dynamics of brain signals, have garnered significant research interest. However, traditional entropy methods like Approximate, Sample, and Fuzzy Entropy are computationally intensive, hindering their application in real-time EEG decoding tasks (Garai et al., 2023). Moreover, relying solely on entropy for criterion weighting can overlook crucial interaction information (Gou et al., 2017; Gou et al., 2020). Vector distance calculation, central to entropy computation, assesses vector similarity in phase space. However, this process is time-consuming, and not all vector pairs require individual distance calculations. Therefore, we introduce a vector dissimilarity algorithm, which directly determines vector dissimilarity, expediting entropy calculations for Sample, Approximate, and Multi-scale Entropy.

Initially, a decision metric, $Decision(i, j) \geq m \times r$, is defined as a sufficient condition for dissimilarity between vectors Xm and Xj(m), as shown in Eq. (5):

$$Decision(i, j) = | \Sigma(k=0 \text{ to } m-1)\ xi+k - \Sigma(k=0 \text{ to } m-1)\ xj+k | \geq m \times r$$

Here, m represents the embedding dimension, and r denotes the similarity tolerance. In Approximate and Sample Entropy calculations, two m-dimensional vectors, Xi(m) and Xj(m), are considered similar if their distance is within r, as shown in Eq. (6):

$$| xi+k - xj+k | < r, \text{ for all } k,\ 0 \leq k \leq m - 1$$

If $Decision(i, j) \geq m \times r$, vectors Xi(m) and Xj(m) are necessarily dissimilar. If two vectors are similar, the absolute difference of their corresponding components is less than $m \times r$, as shown in Eq. (7):

$$\max\{ | xi+k - xj+k | \} < r, \text{ for all } k,\ 0 \leq k \leq m - 1 \implies \Sigma(k=0 \text{ to } m-1) | xi+k - xj+k | < m \times r$$

Based on $Decision(i, j) \geq m \times r$, Eq. (8) can be derived:

$$| \Sigma(k=0 \text{ to } m-1)\ xi+k - \Sigma(k=0 \text{ to } m-1)\ xj+k | \geq m \times r \implies | \Sigma(k=0 \text{ to } m-1)\ (xi+k - xj+k) | \geq m \times r$$

And using $|a| + |b| \geq |a + b|$, Eq. (9) is obtained:

$$\Sigma(k=0 \text{ to } m-1) | xi+k - xj+k | > m \times r$$

Therefore, from Eqs. (6) and (9), vectors Xi(m) and Xj(m) are dissimilar, leading to Eq. (10):

$$\max\{ | xi+k - xj+k | \} > r, \text{ for all } k,\ 0 \leq k \leq m - 1$$

The Decision(i, j) metric thus provides a sufficient condition for vector dissimilarity. By implementing this method, dissimilar vectors are identified directly, bypassing time-consuming distance calculations. Given that dissimilar vectors typically dominate in entropy calculations, this approach significantly enhances computational efficiency.

Dynamic sample entropy is extracted from EEG data using a time window of width tw, moving along the time axis by $\Delta t$. The dynamic sample entropy expression, DySampEn(m, r), is defined for embedding dimension m and similarity threshold r, as shown in Eq. (11) for a brainwave time series of length T:

$$DySampEn(m, r) \langle k \rangle = SampEn(m, r) \langle k \rangle,\ 1 \leq k \leq W$$

Fig. 4 illustrates the emotion valence recognition system. Emotional images are used to elicit emotional responses, and corresponding EEG signals are recorded. After preprocessing and dimensionality reduction, an interactive confirmation method is used to train and test the emotion recognition model. This approach demonstrates strong generalization for cross-individual emotion valence recognition, evaluating performance by testing each participant's EEG against the EEG of others.

Fig. 5 shows the selective attention decoding model based on a deep Long Short-Term Memory (LSTM) network. This model comprises an attentional decoder, a non-attentional decoder, and an attentional classification network, all built upon a 6-layer LSTM Recurrent Neural Network (RNN). The input layer (Level 0) receives EEG, attentional speech envelope, and non-attentional speech envelope sequences. Levels 1-3 consist of parallel attentional and non-attentional decoder modules, each a 3-layer LSTM-RNN structure with a fusion layer. The attentional decoder processes EEG and attentional speech, while the non-attentional decoder processes EEG and non-attentional speech. Levels 4-5 constitute the attention classification module, with two fully connected neural network layers. Level 4 combines the decoder outputs, and Level 5 provides the final classification.

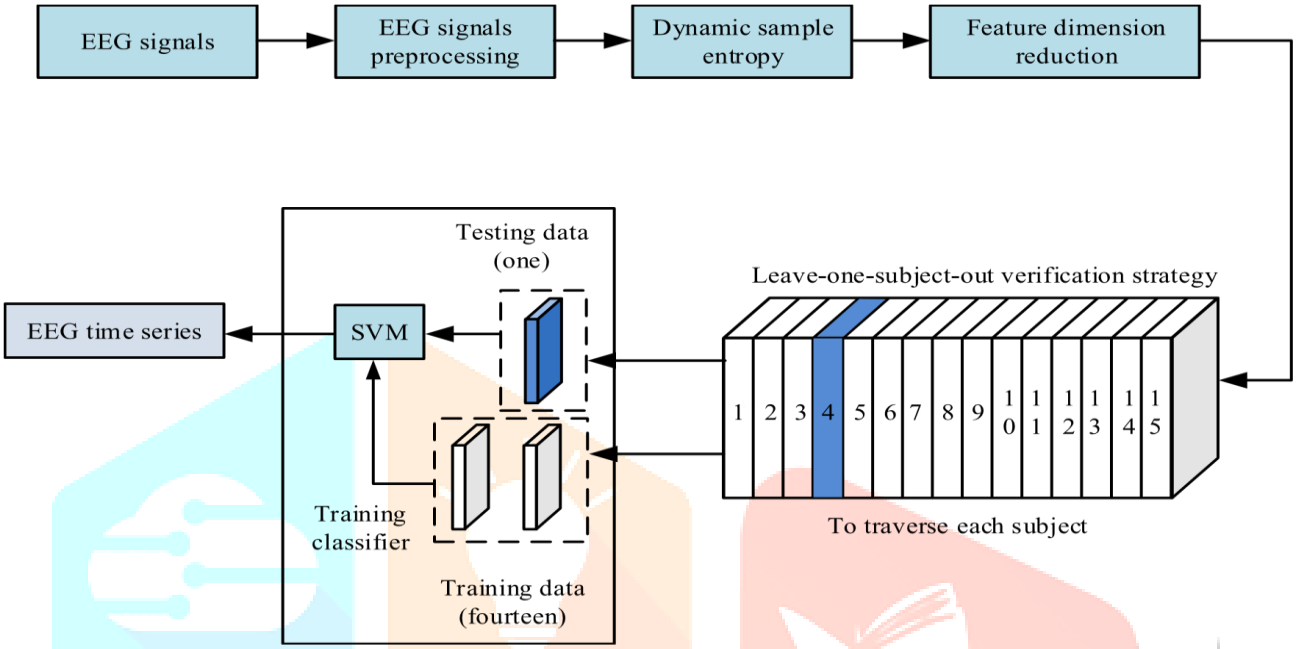


**Fig. 4.** Block diagram of emotion titers recognition system.

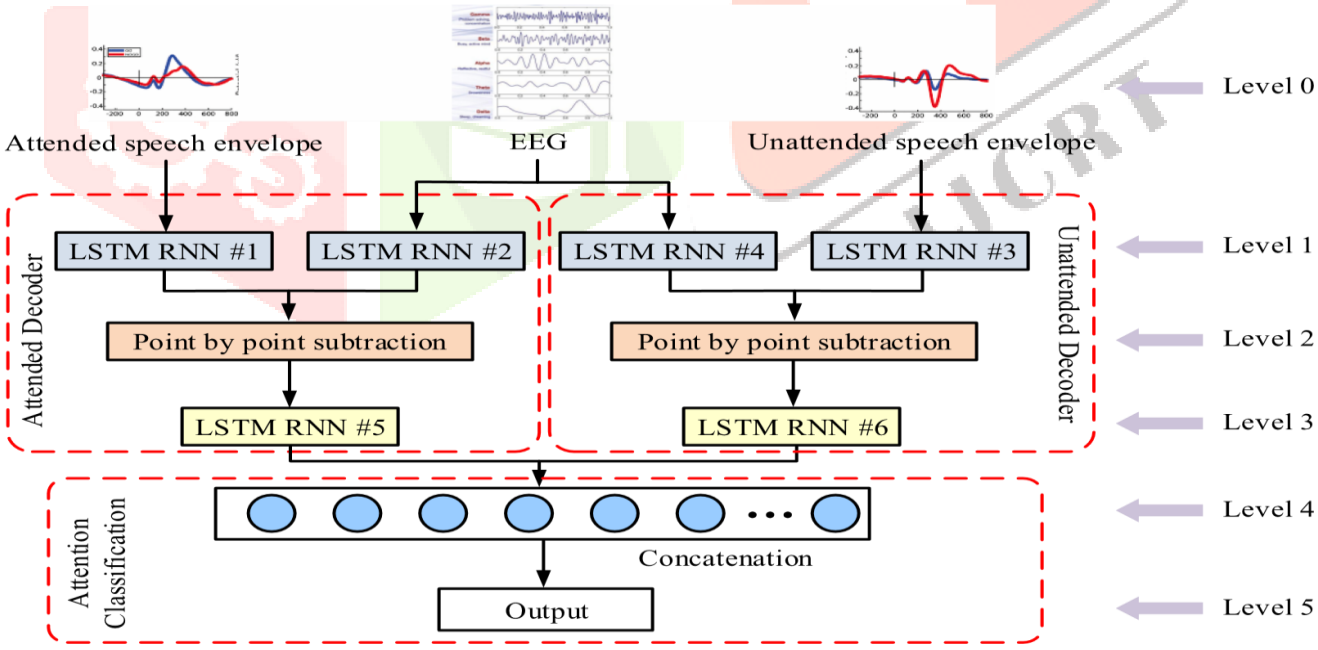


Fig. 5. Selective attention decoding model based on deep LSTM neural network

## 3. Analysis of experimental results

The experiment involved the performance evaluation of the proposed entropy measurement rapid calculation method using simulated signals and real EEG data. Cross-individual emotion state recognition was conducted on 12 participants using the Emotional EEG dataset of Shanghai Jiao Tong University, consisting of 6 males and 6 females (average aged of 26.35±3.64).

### 3.1. Algorithm performance validation:

This study employed video clips designed to elicit positive, negative, and neutral emotional responses, utilizing five clips per emotion category, each lasting approximately four minutes. Participants' emotional states were monitored, and EEG signals were recorded using the ESI-128 EEG acquisition system by Neuroscan. EEG data was collected from 62 channels at a sampling rate of 1000 Hz, with electrode placement adhering to the International Federation of Clinical Neurophysiology standards, as shown in Fig. 6.

Each participant underwent three experimental sessions, spaced at least seven days apart. Each session consisted of 15 trials, resulting in a total of 750 EEG data segments representing the three emotional states, with 225 segments per emotion. EEG data was segmented using a four-second time window, with a two-second overlap between windows. For each channel's EEG time series, 29 sequential entropy features were extracted. The entropy measurement algorithm was implemented in MATLAB, within a computing environment of an Intel Core i7 CPU @ 3.2 GHz with 16GB RAM and Windows 7. The recorded EEG data spanned 60 seconds, sampled at 500 Hz, yielding 30,000 data points. An embedding dimension of 2 and a similarity tolerance of 0.15 were used for entropy calculation.

Fig. 7 presents the computational resource analysis for the proposed algorithm. When processing 100 EEG data segments, the CPU utilization was 26.35%. For 150 segments, CPU usage was 33.75%, and for 225 segments, it was 34.63%. The algorithm consistently maintained low CPU utilization, indicating that system resources were sufficient for data processing.

To evaluate the vector dissimilarity algorithm, a comparison was made against the algorithm detailed in Wen et al. (2023). Table 1 displays the average computation time for multi-scale entropy of EEG signals across varying time intervals (1 to 8). As indicated in Table 1, there are notable differences in computation time between the two algorithms.

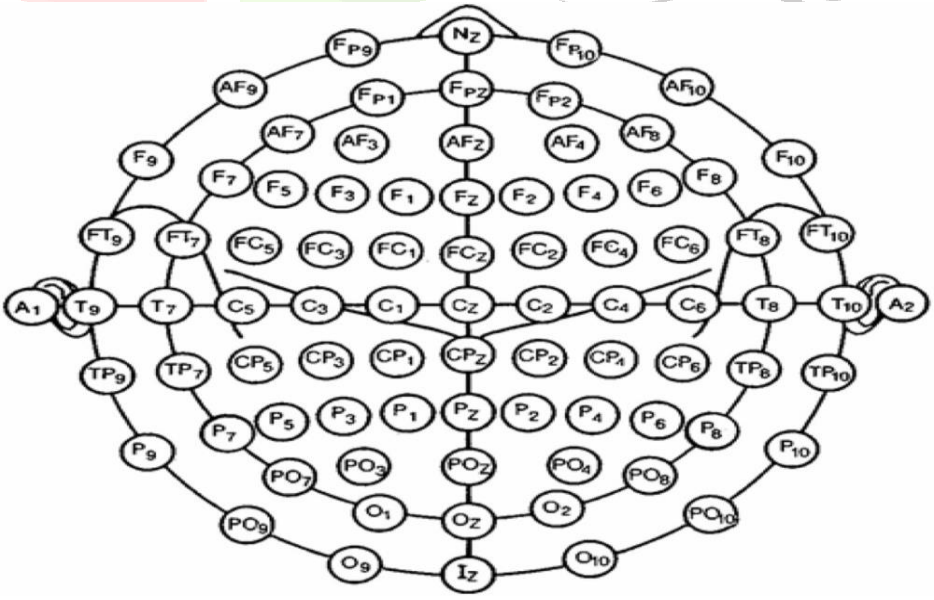


Fig. 6. Schematic diagram of placement of EEG electrodes.

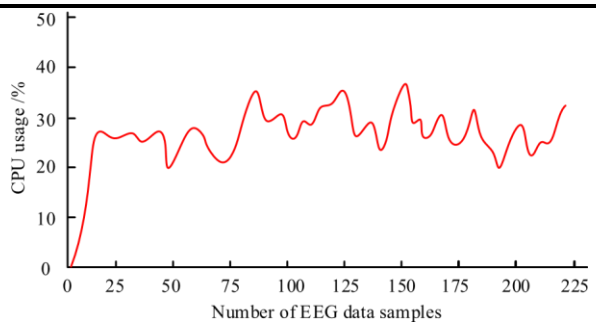


Fig. 7. Computing resources required by the algorithm

The proposed algorithm demonstrated a maximum efficiency improvement of 48.3% and an average improvement of 47.8% compared to the algorithm presented in Li et al. (2023).

To examine the temporal distribution of EEG entropy under varying emotional valences, EEG signals from two participants were analyzed. Fig. 8 displays the time-domain profiles of EEG entropy features, derived from dynamic sample entropy across 29 time windows, for both positive and negative emotional states. In Fig. 8(a), during the first experimental session, entropy values associated with positive emotions were generally slightly higher than those associated with negative emotions. Fig. 8(b) indicates that in the second and third sessions, entropy values for positive emotional states were significantly greater than those for negative states. These findings suggest that the temporal variations in EEG dynamic sample entropy contain information relevant to emotional valence.

For performance validation, three EEG sample conditions were defined: A (attention to animal sounds), B (attention to continuous speech), and Rest (relaxed state with no audio). Complex multi-scale entropy was extracted from 8-channel EEG signals using varying similarity tolerance (r) parameters. Table 2 presents the recognition accuracy for Rest, A, and B using composite multi-scale entropy with r values of 0.1, 0.2, 0.3, and 0.4. The average recognition accuracy was 59.33% ($p = 0.020$) for $r = 0.1$, 70.01% ($p < 0.001$) for $r = 0.2$, 71.29% ($p < 0.001$) for $r = 0.3$, and 55.52% ($p = 0.068$) for $r = 0.4$. The highest recognition accuracy was achieved with $r = 0.3$, resulting in 68.78% for Rest, 77.84% for A, and 67.24% for B.

### 4.2. Recognition Results Analysis

The performance of emotion valence recognition was evaluated across three experimental sessions of EEG data. Table 3 shows the cross-individual positive and negative emotion recognition results using dynamic entropy-based brainwave pattern learning, expressed as mean and standard deviation for 12 participants. The recognition accuracy was 82.66±13.25% for the first session, 82.86±16.35% for the second session, and 82.81±19.08% for the third session, with an overall average accuracy of 82.78±16.22%. The average recognition accuracy for positive and negative emotions across all tests was

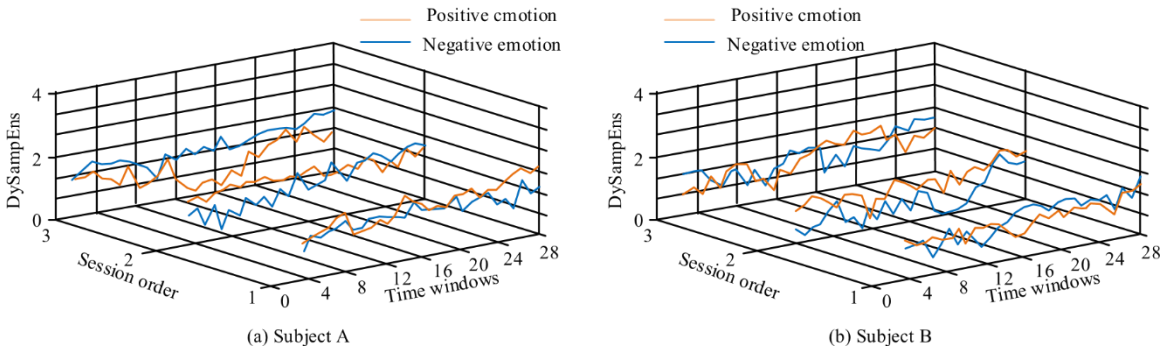

Results of multi-scale entropy identification using different similarity tolerance parameters.

| Recognition rate | Similarity tolerance *r* | | | |
|---|---|---|---|---|
| | 0.1 | 0.2 | 0.3 | 0.4 |
| Rest | 63.25 % | 69.85 % | 68.78 % | 55.17 % |
| A | 61.76 % | 77.18 % | 77.84 % | 62.23 % |
| B | 52.97 % | 63.01 % | 67.24 % | 49.17 % |
| Average recognition rate | 59.33 % | 70.01 % | 71.29 % | 55.52 % |

**Table 3**

Resultsofemotionrecognition.

| Experiment round | 1 | 2 | 3 | Mean value |
|---|---|---|---|---|
| Accuracy rate (%) | 82.66 ±13.25 | 82.86 ±16.35 | 82.81 ±19.08 | 82.78 ±16.22 |
| Sensitivity (%) | 82.36 ±24.66 | 86.94 ±24.63 | 80.16 ±18.95 | 83.15 ±22.75 |
| Specificity (%) | 82.91 ±20.36 | 78.81 ±31.68 | 85.92 ±27.65 | 82.55 ±25.36 |
| Error rate (%) | 18.63 ±13.79 | 17.63 ±16.84 | 17.65 ±18.45 | 17.97 ±16.36 |
| Sample size | 150 | 150 | 150 | 450 |

The recognition accuracy across the three experimental sessions showed a high degree of consistency. This indicates that the dynamic entropy-based brainwave emotion pattern learning method is capable of robust cross-individual emotion valence recognition.

Fig. 9 presents the cross-individual emotion recognition results for the 12 participants across the three experimental sessions. As shown in Fig. 9(a), the individual accuracy rates were 86.67%, 66.67%, 83.33%, 80.00%, 63.33%, 90.00%, 86.67%, 100%, 70.00%, 80.00%, 100%, and 76.67%, respectively. The average accuracy was 84.64% ± 11.38%, demonstrating improved performance compared to the single-round experiments. This enhancement can be attributed to the general trend of learning algorithms improving with increased data samples.

Fig. 9(b) illustrates the recognition results for positive, negative, and neutral emotions across the 12 participants. The individual accuracy rates were 60.00%, 55.56%, 73.33%, 66.67%

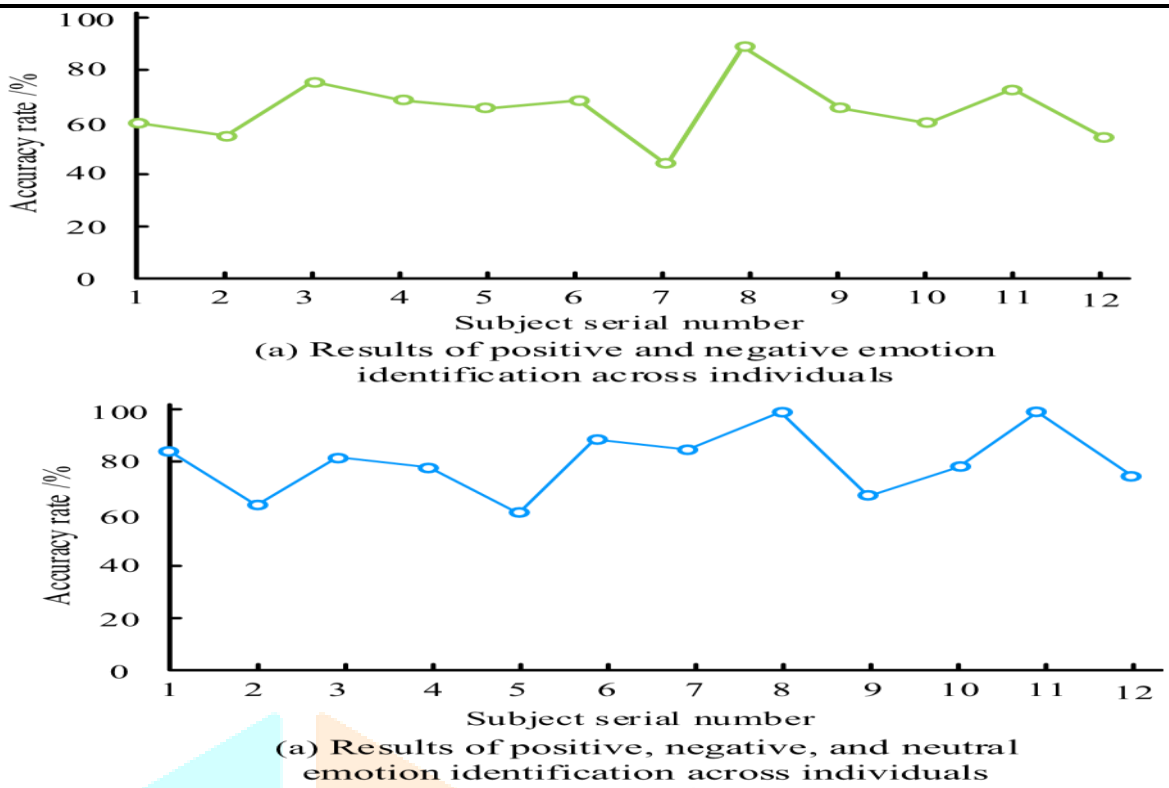


**Fig. 9.** Results of emotion recognition based on dynamic entropy pattern learning.

The recognition accuracy for positive, negative, and neutral emotions across the 12 participants was: 60.00%, 55.56%, 73.33%, 66.67%, 64.44%, 66.67%, 46.67%, 84.4%, 64.44%, 60.00%, 75.11%, and 55.56%, with an average accuracy of 60.98%

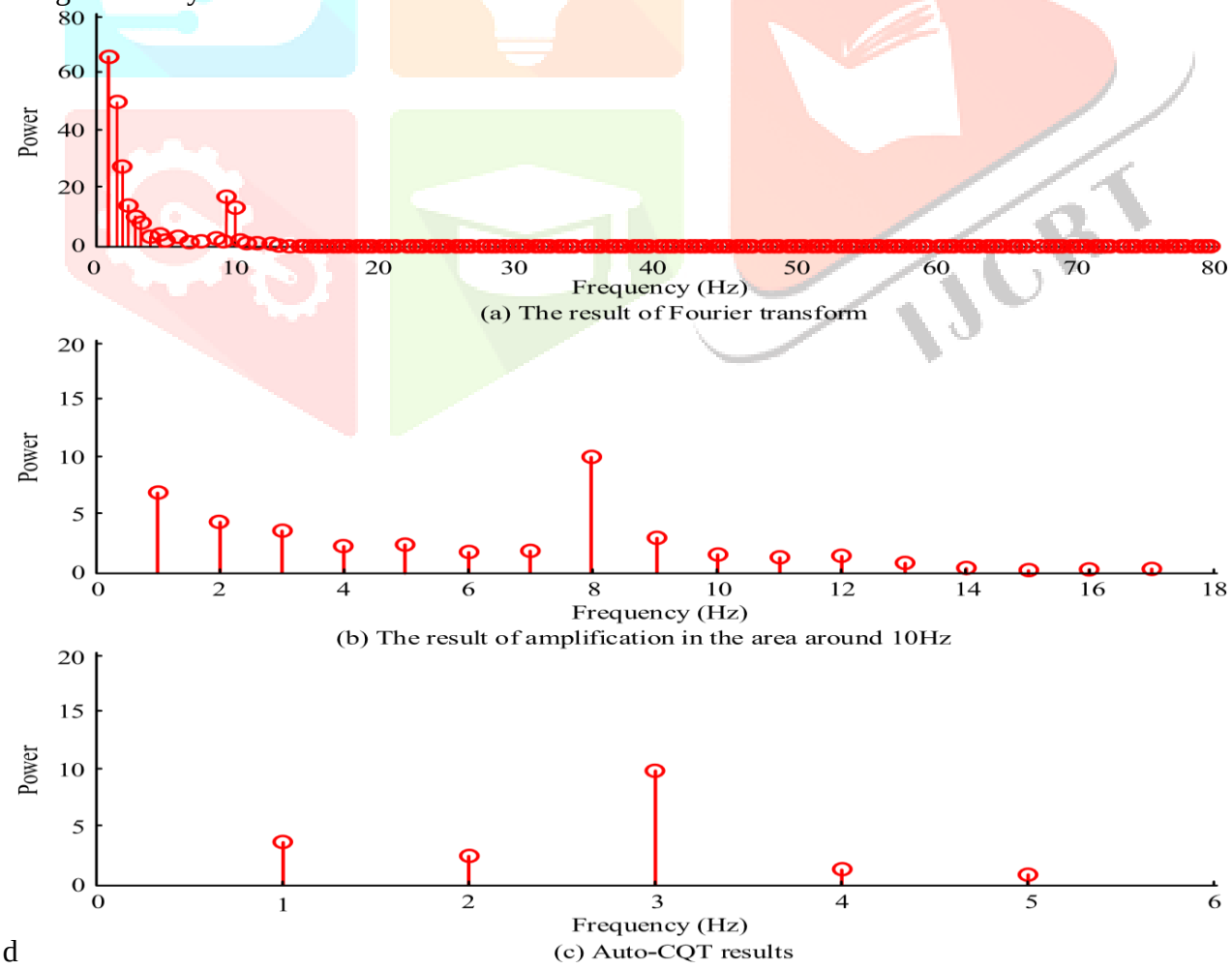


d

Fig. 10. EEG Spectrum Analysis Results

This research employed Fourier transform, Classical Constant Q Transform (Classic-CQT), and Automatic Constant Q Transform (Auto-CQT) to analyze EEG signals and determine the percentage of the α frequency band. The Fourier transform calculated total band power by summing electrode spectral powers due to its wider bandwidth at higher frequencies. CQT, on the other hand, averaged electrode spectral powers for each band. Fig. 10(a) showed the Fourier transform results, revealing a significant amplitude at 10 Hz, but with notable amplitudes in adjacent spectral lines. Fig. 10(b) provided a magnified view of the 10 Hz range from Fig. 10(a). Fig. 10(c) presented the Auto-CQT results, demonstrating that CQT spectral lines provided more distinct spectral features.

The auditory selective attention encoding model, based on Long Short-Term Memory (LSTM) deep networks, was trained and tested using samples of nine different lengths. Fig. 11(a) illustrated that sound recognition accuracy for auditory attention targets was consistently high across participants when sample durations were below 1.5 seconds. However, with durations exceeding 2 seconds, significant variations in target word recognition accuracy were observed. The median accuracy for auditory attention targets remained relatively consistent across varying sequence lengths, as shown in the box plot of Fig. 11(a). Fig. 11(b) demonstrated the relationship between accuracy and the number of model training cycles. Recognition accuracy reached approximately 50% after 5 training cycles, indicating insufficient training. As training cycles increased from 5 to 40, recognition rates significantly improved. With over 45 training cycles, the LSTM-based auditory selective attention decoding model achieved approximately 95% prediction accuracy.

To evaluate the impact of different brain regions' EEG information features on emotion valence recognition, brain electrodes were partitioned, as shown in Fig. 12(a). The partitions included left and right frontal, left and right posterior, and left and right hemispheres, as well as anterior and posterior regions. The recognition performance of positive and negative emotions across individuals was analyzed for eight brain region partitions, with results shown in Fig. 12(b). Using EEG data from 15 participants, the accuracy of emotion valence recognition, based on the dynamic entropy-based EEG emotion map learning algorithm, was 84.36%, 70.65%, 78.44%, 80.12%, 70.08%, 69.94%, 80.23%, and 74.63%, respectively, corresponding to the frontal hemisphere, posterior hemisphere, left hemisphere, right hemisphere, left posterior region, right posterior region, left frontal lobe, and right frontal lobe regions. Despite having only 33 EEG electrodes, the anterior hemisphere showed the highest accuracy (84.36%) in emotion valence judgment, indicating the importance of brain region and electrode channel selection. The EEG activity in the anterior hemisphere may contain the most relevant information for emotion valence judgment.

To compare with other emotion recognition systems, various algorithmic models were tested on datasets, and algorithms such as Discrete Wavelet Transform (DWT), Empirical Mode Decomposition (EMD), and Short-time Fourier Transform (SFT) were reproduced for comparison. The test results for each participant are shown in Fig. 13. The data were divided into 10 equal segments, and ten-fold cross-validation was conducted for each participant's data.

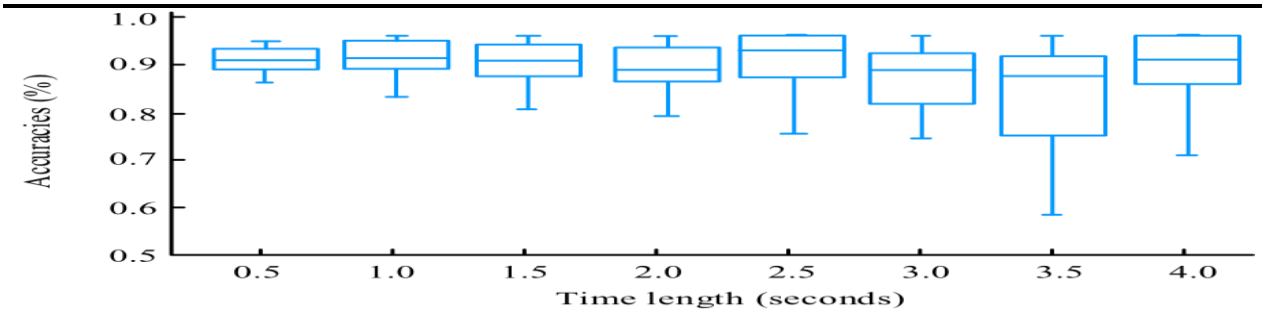


(a) The influence of sample sequence length on decoding performance

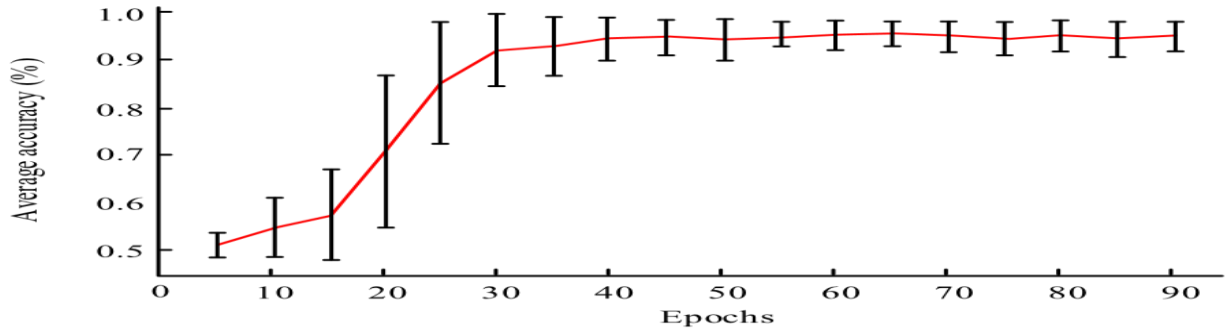


(b) The influence of the number of training rounds on decoding performance

The proposed method achieved an average recognition accuracy of 92.19%, compared to 85.51% for Discrete Wavelet Transform (DWT), 83.75% for Empirical Mode Decomposition (EMD), and 86.27% for Short-time Fourier Transform (SFT). The proposed method demonstrated an accuracy improvement of over 5% compared to these alternative algorithms. Furthermore, it outperformed baseline methods in cross-individual emotion titer recognition. This improvement is attributed to the input feature vector, which utilizes the time-domain contour of dynamic sample entropy, derived from a sliding time window. This approach effectively captures the temporal dynamics of EEG entropy, representing the temporal state characteristics of emotions and enhancing the representation of emotion-related EEG activity. Consequently, the dynamic entropy-based EEG emotional pattern learning method provides more accurate monitoring of emotional states from EEG signals, improving inter-individual emotion tier recognition.

Table 4 compares the proposed method with existing studies. The proposed method showed superior recognition rates for Rest and A tasks in the 3-classification auditory target recognition scenario. While the performance for task B was not the highest, it was comparable to existing research. These results demonstrate the effectiveness of EEG entropy measures in extracting brain activity information related to auditory target attention from EEG signals. By constructing an auditory attention classifier using machine learning, the model learns patterns and rules from EEG entropy feature data, enabling emotion recognition based on EEG signals. Notably, the proposed model achieved high-precision auditory selective attention decoding using only eight EEG channels, a significant reduction compared to other methods. This reduction in EEG decoding signal requirements, such as time series duration and channel count, enhances the practical value of the approach. A key limitation of existing auditory selective attention decoding methods, particularly stimulus reconstruction methods, is their reliance on excessively long EEG time series, which restricts their practical application. Therefore, the proposed auditory attention decoding method offers a promising direction for future research and development.

## 4. Conclusion

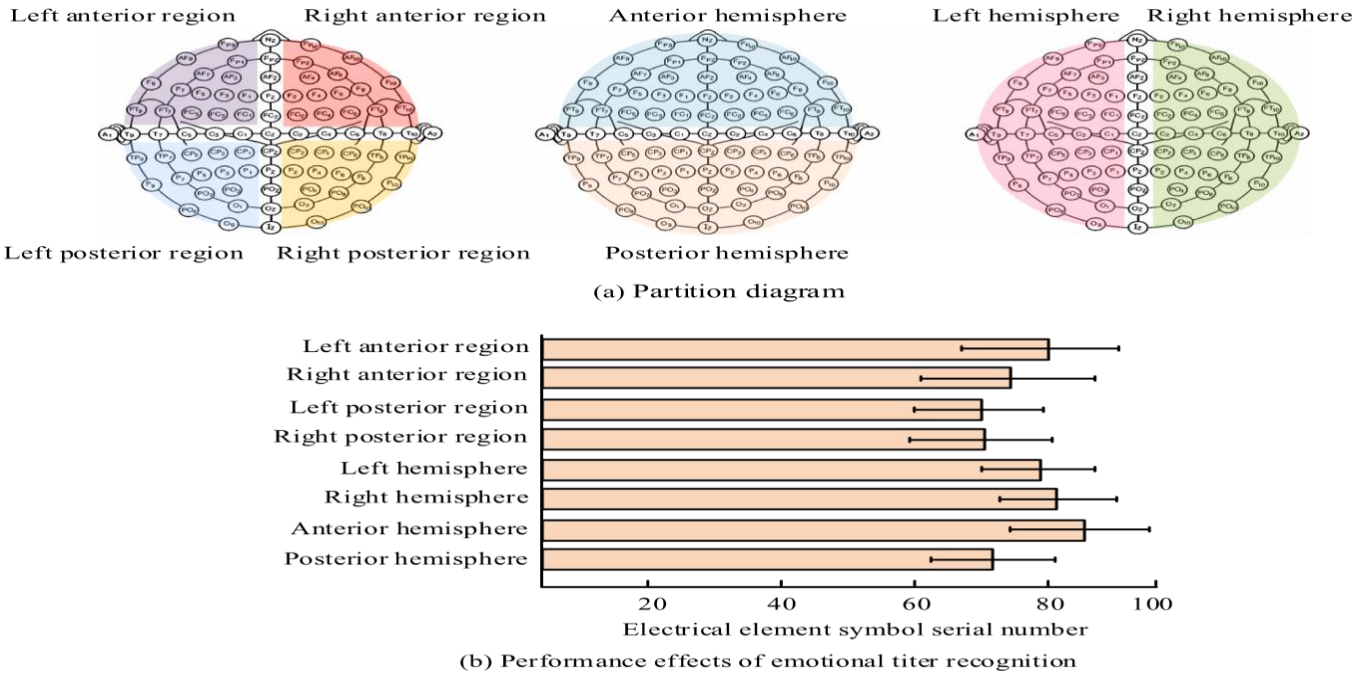


This study focused on recognizing individual psychological and emotional states by integrating time-series decomposition and reconstruction with EEG entropy measures. An EEG signal decoding method was developed, combining Singular Spectrum Analysis (SSA) and entropy measures. To address the computational demands of entropy calculations, a vector dissimilarity criterion was implemented to expedite the process. The results indicated that this SSA-entropy based EEG decoding method effectively improved EEG decoding performance. Compared to the algorithm in Wen et al. (2023), the accelerated entropy calculation method demonstrated a 47.8% increase in computational efficiency.

The proposed EEG emotion recognition method achieved a peak recognition accuracy of 84.64% for positive and negative emotional states, and 64.15% for cross-individual positive, neutral, and negative states. The average emotion recognition accuracy across three experimental sessions was 82.78±16.22%. The consistency of recognition accuracy across these sessions highlighted the robustness of dynamic entropy-based EEG emotional pattern learning for cross-individual emotion valence recognition. The proposed method achieved an average accuracy of 92.19% on the SEED dataset, outperforming Discrete Wavelet Transform (DWT), Empirical Mode Decomposition (EMD), and Short-time Fourier Transform (SFT) algorithms by over 5%.

The developed EEG decoding method proved effective in processing EEG signals with non-stationary, nonlinear, and multi-component characteristics, showing enhanced cross-individual emotion recognition and improved generalization. This cognitive computing method for cross-individual emotional state recognition optimized EEG emotional pattern recognition, enabling effective prediction of psychological and emotional states from EEG signals. Comparisons with Li et al. (2023) and Kamble & Sengupta (2023) demonstrated the method's ability to learn emotional features from EEG entropy data.

However, EEG signal collection can be affected by disturbances like EMG artifacts, potentially reducing emotion recognition accuracy. Future work will explore adaptive filters to dynamically adjust parameters based on EEG signal and noise statistics, enhancing signal-to-noise ratio and overall performance.

## 5.References


Althobaiti, M. M., Kumar, K. P. M., Gupta, D., Kumar, S., & Mansour, R. F (2021). An intelligent cognitive computing based intrusion detection for industrial cyberphysical systems. *Measurement, 186*(2), 110145.1-110145.9.

Aryavalli, S. N. G., & Kumar, G. H (2023). Futuristic vigilance: Empowering chipko movement with cyber-savvy IoT to safeguard forests. *Archives of Advanced Engineering Science, 1*(8), 1–16.

Cao, H., Wu, Y., Bao, Y., Feng, X., Wan, S., & Qian, C. (2023). UTrans-Net: A model for short-term precipitation prediction. *Artificial Intelligence and Applications, 1*(2),
106–113.

Cui, H., Liu, A., Zhang, X., Chen, X., Wang, K. Q., & Chen, X. (2020). EEG-based emotion recognition using an end-to-end regional-asymmetric convolutional neural network.
*Knowledge-Based Systems, 205*(12), 106243.1-106243.9.

Garai, S., Paul, R. K., & Kumar, M. (2023). Intra-annual national statistical accounts based on machine learning algorithm. *Journal of Data Science and Intelligent Systems, 2*(2), 12–15.

Ghasemi, M., Zare, M., Zahedi, A., Akbari, M., Mirjalili, S., & Abualigah, L. (2024). Geyser inspired algorithm: A new geological-inspired meta-heuristic for realparameter and constrained engineering optimization. *Journal of Bionic Engineering,*
*21*(1), 374–408.

Goshvarpour, A., & Goshvarpour, A. (2022). Schizophrenia diagnosis by weighting the entropy measures of the selected EEG channel. *Journal of Medical and Biological Engineering, 42*(6), 898–908.

Gou, X., Xu, Z., & Liao, H. (2017). Hesitant fuzzy linguistic entropy and cross-entropy measures and alternative queuing method for multiple criteria decision making.
*Information Sciences, 388*, 225–246.

Gou, X., Xu, Z., Liao, H., & Herrera, F. (2020). Consensus model handling minority opinions and noncooperative behaviors in large-scale group decision-making under double hierarchy linguistic preference relations. *IEEE Transactions on Cybernetics, 51* (1), 283–296.

Hrisca-Eva, O. D., & Lazar, A. (2021). Multi-sessions outcome for EEG feature extraction and classification methods in a motor imagery task. *Traitement du Signal, 38*(2),
261–268.

Kamble, K. S., & Sengupta, J. (2023). EVNCERS: An integrated eigenvector centralityvariational nonlinear chirp mode decomposition-based EEG rhythm separation for automatic emotion recognition. *IEEE Sensors Journal, 23*(18), 21661–21669.

Kim, D. H., Park, J. O., Lee, D. Y., & Choi, Y. S (2024). Multiscale distribution entropy analysis of short epileptic EEG signals. *Mathematical Biosciences and Engineering, 21* (4), 5556–5576.

Li, H., Wang, G., Lu, J., & Kiritsis, D. (2022). Cognitive twin construction for system of systems operation based on semantic integration and high-level architecture.
*Integrated Computer-Aided Engineering, 29*(3), 277–295.

Li, Q. L., Zhang, T., Chen, C. L. P., Yi, K., & Chen, L (2023). Residual GCB-Net: Residual graph convolutional broad network on emotion recognition. *IEEE Transactions on Cognitive and Developmental Systems, 15*(1), 1673–1685.